IRAQI JOURNAL OF APPLIED PHYSICS
Vol. 22, No. 3, July-September 2026, pp. 358-372

Sustainable UPE Composites Reinforced with Recycled HDPE: Correlation of Mechanical, Thermal, and Acoustic Performance

Saad M. Hashim*
Waleed B. Salih

Department of Physics,
College of Education for Pure Science,
University of Anbar,
Ramadi, 31001, IRAQ
* Corresponding author email:
saa23u3001@uoanbar.edu.iq

This paper produces environmentally friendly unsaturated polyester resin (UPE) composites that use finely ground high-density polyethylene (HDPE) particles (approximately 53 μm, 0-10 wt.%). Mechanical, thermal and acoustic properties were assessed systematically in order to identify structure property relationships. Incorporation of HDPE enhanced compressive strength (56.6→94.4 MPa), impact resistance (+70%), surface hardness (75.4→80.5 Shore D), thermal conductivity (0.19→0.26 W/m^2.°C), and sound insulation (≈ 20 dB reduction at 10 kHz). On the other hand, flexural strength declined (>80%). FTIR was used to confirm the chemical stability of the recycled HDPE following remelting, whereas microscopy was used to identify homogeneous dispersion of the reinforcing particles as the cause of enhanced damping and toughness. The results indicate the possibility of using recycled HDPE as a versatile filler that could allow creating lightweight, low cost, and environmentally-friendly UPE composites used in acoustical and energy-absorbing applications.

Keywords: Polymer composites; Mechanical properties; Acoustical materials; Heat conduction
Received: 31 August 2025; Revised: 24 November; Accepted: 1 December; Published: 1 July 2026

1. Introduction

The mass of plastics in the world has rendered it significant that people consider green materials, particularly the methods of recycles and re-using commonly utilized polymers such as high-density polyethylene (HDPE) and polyethylene terephthalate (PET). The plastics used in packaging and consumer goods are a big source of post-consumer waste [1, 2]. Waste can be used to create composite materials which is a great idea for the environment since it fits the circular economy and helps limit our dependence on newly produced polymers [3-5].

Recycled HDPE has been found to be a good reinforcement of UPE since it is mechanically strong, resistant to heat. Several studies have shown that composite constructions of HDPE and recycled PET fibers or flakes could significantly improve mechanical properties, including tensile, flexural and impact strength [6-8]. This can further be improved by adding compatibilizers such as maleic anhydride grafted polyethylene (PE-g-MA) since they increase the interfacial bonding and compatibility of two polymers [9, 10].

Teixeira and Moraes (2023) state that post-consumer PET/HDPE blends are more crystalline and possess better thermal properties, thus can serve as HDPE substitutes [2]. In terms of their properties, researchers have paid attention to the capability of these composites to insulate against sound, primarily in structural beams, and they also serve to absorb sound within the middle to high-frequency range [11].

The addition of different natural and mineral fillers into HDPE composites can contribute to faster sustainable material development. It has been found that with the inclusion of diatomaceous earth, either alone or in combination with new reversible crosslinking reaction agents (RXR), mechanical strength and crystallinity can be improved, and the processability and thermal behavior can be improved as suggested in a paper by Reguig et al. (2024) [12]. Similarly, incorporation of fly ash cenospheres into HDPE has enhanced tensile strength, flexural strength, modulus and heat resistance, so these composites are very appropriate in the construction of different infrastructure such as drainage pipes and support panels [13, 14]. Banana fibers and wood flour are popular in composites as natural reinforcing materials because they are biodegradable, low-cost and have good mechanical properties. The use of banana fiber and peels in HDPE has strengthened the material, improved its resistance to heat and reduced its environmental impact [15-17]. In addition, when wood fibers are chemically modified with maleated coupling agents, they are strongly attached to HDPE, leading to improved flexibility, higher tensile values and better heat resistance [18, 19]. For special purposes such as marine equipment and food packaging, HDPE composites are modified with crosslinking and mixed with fillers (for example, diatomaceous earth and zinc oxide) to provide needed features such as resistance to ultraviolet light, anti-bacterial effects and strong structure [20-24].

Given this context, the current study presents a novel approach by incorporating finely ground recycled HDPE particles (53 μm), derived from post-consumer plastic waste, as a reinforcement in unsaturated polyester resin (UPE) composites at varying weight fractions (0%, 2.5%, 5%, 7.5%, and 10%). The main

objective of the current research is to clarify the physicomechanical processes by which compressive, impact, thermal, and acoustic properties can be improved concurrently in UPE/HDPE hybrid systems. This is driven by the necessity to heroise post-consumer HDPE to high performance thermoset composites and to elucidate the interfacial and microstructural determinants of property trade-offs, especially the differences in flexural failure behaviour.

2. Materials and Methods

In this study, the unsaturated polyester resin (UPE) employed is an ortho-phthalic based resin formulation provided by Saudi Industrial Resins (SIR), which has a medium density crosslinking and polar ester groups which affect the adhesion characteristics of the bonding agent with non-polar HDPE particles. The resin, produced by Saudi Industrial Resins (SIR), has its viscous transparent pink appearance at ambient temperature. UPE being a thermosetting polymer, it hardens irreversibly through crosslinking when a chemical initiator is added.

Methyl ethyl ketone peroxide (MEKP) was used as the curing agent, introduced at a ratio of 2 parts per 100 parts of resin by weight. Polymerization commenced at room temperature (~25 °C), generating an exothermic reaction that transformed the resin into a rigid, three-dimensional polymer network. The material specifications for the UPE resin, as provided by the supplier, are listed in table (1).

Table (1) Thermo-physical properties of UPE resin

Property	Value Range
Elastic Modulus (GPa)	2.06 – 4.41
Specific Heat Capacity (J/kg.K)	710 – 920
Thermal Conductivity (W/m.°C)	0.17
Density (g/cm^3)	1.20

The reinforcement employed in this experiment was of a recycled HDPE which was based on post-consumer sources of plastic-packaging containers and house waste materials (Fig. 2a). The obtained HDPE was washed, heated, and milled into a fine powder with a controlled particle size of about 53 µm.

HDPE is a semi-crystalline thermoplastic with high toughness, zero water solubility, and chemical inertness, which are the qualities that make it a very effective additive in enhancing both mechanical strength and acoustic damping in polymer composites. Table (2) summarizes the key properties of the HDPE material used.

Recycled HDPE was then sequentially treated physically where it was first cut into smaller pieces using a mechanical cutter (Fig. 1a). These fragments were then thermally melted at 150C in a lab-scale furnace and then allowed to cool in the ambient temperature. To obtain a fine particulate powder of mean diameter of 53 µm the solidified polymer was ground in a high-speed grinder to a fine particulate powder as demonstrated in Fig. (1b).

Table (2) Physical and chemical attributes of HDPE

Property	Value Range
Chemical Formula	C_2H_4
State	Solid
Density (g/cm^3)	0.95 – 0.98
Water Absorption	0
Appearance	Multi-color

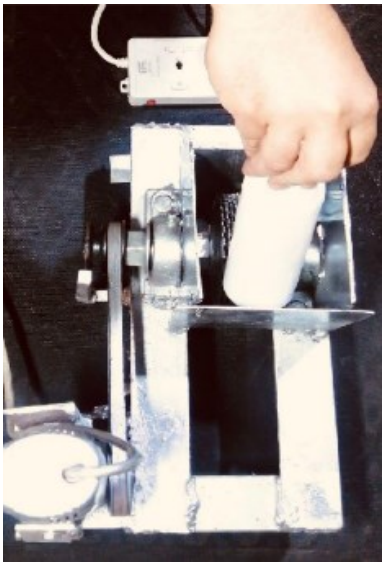

(a)

(b)

Fig. (1) (a) Mechanical cutting of recycled HDPE bottles into small fragments, and (b) HDPE final powder obtained from melting, cooling, and grinding (average particle size of 53 µm)

Specimens were manufactured via the manual hand lay-up technique, a conventional method for fabricating thermoset-based composite panels. Aluminum and glass molds were employed to shape the specimens according to standardized test dimensions. The HDPE filler was incorporated into the UPE matrix at predetermined weight fractions of 0%, 2.5%, 5%, 7.5%, and 10%.

HDPE particles were incrementally added to the UPE resin and manually stirred using a glass rod until a visually homogeneous mixture was achieved. MEKP hardener was then blended into the mixture in a fixed ratio of 2 g per 100 g of resin, followed by casting into molds and curing under ambient conditions.

The weight fraction of the HDPE reinforcement was determined using the following relationships [25]:

$$\Psi = \left(\frac{w_p}{w_c}\right) \times 100 \quad (1)$$

$$w_c = w_p + w_m \quad (2)$$

where Ψ is the weight percentage of HDPE, W_p is the weight of HDPE filler, W_m refers to the weight of UPE matrix, and W_c is the total weight of the composite system.

This method ensured reproducibility in sample preparation across all test groups. The fabricated specimens were subsequently characterized through mechanical testing, FTIR spectroscopy, thermal conductivity analysis, and acoustic insulation evaluation

The flexural properties of the UPE/HDPE composites were measured using a three-point bending test according to ASTM D790-23 [26]. A LARYEE Yaur Testing Solution universal testing machine was used for the testing. Every specimen was held at both supporting points as a load was applied in the middle to induce bending stress until it failed. Flexural strength which is another name for modulus of rupture, refers to the maximum stress that the test specimen endured just before breaking. The test revealed important information about how increasing the HDPE particle content in the composite affects its ability to resist bending. It provided a visual understanding of failure types (such as surface cracking or fracture in the middle) depending on the filler percentage used. Images of the tested specimens before and after test can be viewed in Supplementary Fig. (S1).

Evaluating compressive strength was performed for all composite formulations following the standards in ASTM D695-23 [27]. The same testing machine (LARYEE Yaur Testing Solution) applied an axial force to the samples which were positioned vertically between two flat compression plates. After testing with a specific load, the load was increased gradually each time until either the material broke or was deformed greatly. The compressive strength of the sample was determined by determining the maximum pressure that the sample could withstand before collapsing or yielding. The knowledge of the measurement aids us to assess the effect of addition of HDPE on the resistance of the material to axial forces which is critical in the construction and engineering practice. Although the compressive modulus was not evaluated, the test data on strength show how the composite construction can sustain loads and react to HDPE reinforcement. Supplementary Figure (S2) shows images of the tested specimens prior to and after test.

The Charpy impact test was conducted on the UPE/HDPE composites, using the protocol mentioned in ASTM D6110-18 [28]. Experiments were performed on specimens (4 mm wide, 10 mm thick and 80 mm high). Testing was conducted using a Charpy impact tester fitted with a 7 J calibrated pendulum. The test involved positioning each specimen horizontally and letting it be struck by the swinging pendulum at its center. At the moment of fracture, the equipment registered and indicated the energy taken in kJ /m² which is the strength of the material being pressured unexpectedly. Three samples were analyzed to obtain the data of each content level of HDPE to ensure the statistical accuracy. This method made it possible to evaluate how adding different levels of HDPE affected the toughness and impact strength of the composite. Images of the tested specimens before and after test can be viewed in Supplementary Fig. (S3).

Surface hardness was measured using the Shore D scale as outlined in ASTM D2240-15 [29]. A digital Shore D durometer (Elcometer 120, UK) was used to evaluate the indentation resistance of the cured UPE/HDPE composites. The indenter applied a perpendicular force to various surface locations, and the Shore D hardness values were read directly from the device's digital gauge. For each sample, hardness readings were taken at three different surface points and the average value was shared as the hardness result. With these tests, we were able to see how the properties of the material's surface, wear resistance and resistance to permanent deformation changed as the HDPE concentration was raised. Images of the tested specimens before and after test can be viewed in Supplementary Fig. (S4).

Each reported mean value represents three independent specimens (n=3). Although sample number was limited by fabrication constraints, standard deviations were <5% for all mechanical tests, indicating good repeatability. An ANOVA test confirmed that variations between successive HDPE loadings were statistically significant at $p < 0.05$.

The thermal conductivity of the UPE/HDPE composite samples was determined using the Ta Lee disk method with the help of a Griffen & George thermal conductivity apparatus. The device consisted of circular discs made of copper, each 50 mm in diameter and 5 mm in thickness, to enclose the test sample in the center. A constant electric current of 0.25 A at a voltage of 6 V was applied to establish steady-state heat flow through the sample configuration. Images of the tested specimens before and after test can be viewed in Supplementary Fig. (S4).

Temperature readings were obtained from three distinct copper plates—denoted as TA, TB, and TC—corresponding to the top, middle, and bottom thermal contact interfaces, respectively. The heat input and thermal conductivity were computed using the following expressions [30]:

$$K\left(\frac{T_B - T_A}{T_S}\right) = e\left[T_A + \frac{2}{r}\left(d_A + \frac{1}{4}d_s\right)T_A + \frac{1}{2r}d_S d_B\right] \quad (3)$$

$$H = IV = \pi r^2 e(T_A + T_B) + 2\pi re\left[d_A T_A + d_s \cdot \frac{1}{2}(T_A + T_B) + d_B T_B + d_C T_C\right] \quad (4)$$

where K is the thermal conductivity of the composite (W/m·°C), e refers thermal energy transfer rate (W/m²·°C), H is the heat power input (W), T_A, T_B, T_C

refer to the temperatures at each copper interface (°C), d_A, d_B, d_C denotes to the thicknesses of copper plates (mm), ds is the sample thickness (mm), r is the disc radius (mm), I is the current (A), and V is voltage (V)

This method enabled the proper identification of the conducting capacity of the composite and gave significant information about whether the composite can be applied in thermal management or insulating systems.

The stability of the chemical bonds and the structure of the HDPE within the polyester matrix was analyzed using Fourier-transform infrared (FTIR) spectroscopy. Spectral analysis was also conducted prior to and after thermal processing to find out whether there was any alteration in chemical bonding or functional groups which may affect the performance of the composite.

Measurement was done with the help of a high-sensitivity detector and an integrated digital signal processor using a PerkinElmer Spectrum Two FT-IR spectrometer. To obtain good spectral quality and signal to noise ratio, the IR spectra were recorded in the mid infrared region (400 to 4000 cm^{-1}) at 16 scans per sample on average. The composites were analyzed by laying the composites as thin-films and viewing the samples under transmission mode. Three equal specimens in the content of HDPE were subjected to all tests that were done to ensure that findings are reliable.

All the experiments mentioned such as tensile, compression, flexure, impact strength, hardness and thermal conductivity testing, were set up and performed at the Advanced Materials Laboratories in the Department of Physics, College of Education for Pure Sciences. All tests were conducted according to the required ASTM testing standards, making sure the data collected was accurate and could be repeated. All equipment was calibrated and the laboratory was kept at a controlled temperature and humidity before any measurements were taken to ensure accurate results. In parallel, we gathered data using Fourier-transform infrared (FTIR) spectroscopy at the Department of Chemistry, in this college.

Optical microscopy is a fundamental analytical technique in materials characterization, as it enables the visualization of microstructures and surface features that are not visible to the naked eye. It allows researchers to see the surface structures and internal forms of composite materials clearly. Structural and surface analysis in many industries depend on the use of optical microscopes. To study surface and cracks, this research used an optical microscope which is a binocular, electrically powered unit manufactured by Nikon, Japan, equipped with a pair of 10× eyepieces and three objective lenses (4×, 10×, and 40× magnification). The microscope is equipped with a 20 W halogen illumination source, providing consistent lighting and high image clarity across all magnifications.

Acoustic insulation testing was used to study how effective the UPE/HDPE composites are at blocking the passage of airborne sound at different frequencies. This test identifies the capabilities of polymer material in the use of noise control such as construction sound barrier, sound enclosures and motor interior insulation.

The acoustic tests (see Fig. 2) were conducted in a controlled acoustic chamber system using a fixed reverberation chamber system whereby each specimen of composite acted as a barrier between a controlled sound source and an array of receivers. The incident sound power level (SPL) was kept at around 120 dB produced by a high precision loudspeaker fed directly by a signal generator and power amplifier. According to the ISO 10534-2 standards, calibration of SPL was carried out on a reference microphone and a Class 1 digital sound-level meter (precision within 0.5 dB). Such arrangement was able to maintain a stable and repeatable incident sound field in all tests. The chamber was acoustically enclosed to reduce the background noise, reflections, and environmental interference and guarantee reliable measurement of the sound transmitted levels through the measured frequency range.

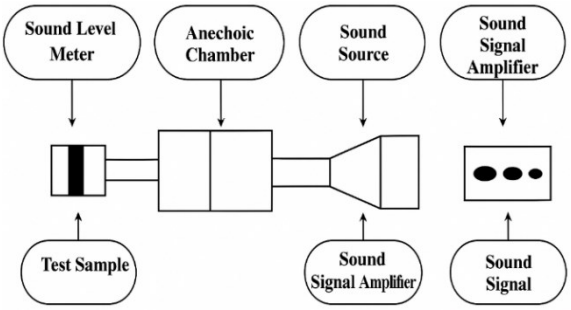

Fig. (2) Schematic representation of the acoustic insulation testing setup used to evaluate sound transmission through UPE/HDPE composite

The acoustic performance was determined at three common frequencies 100 Hz (low-frequency), 1000 Hz (mid-frequency) and 10,000 Hz (high-frequency) depending on the common frequencies in residential and industrial setting. Each of the three compositions with HDPE at 0, 2.5, 5, 7.5, and 10 percent by weight was measured at the SPL.

Three distinct measurements at each frequency were made on each formulation to ascertain the statistical accuracy. The average level of sound (in decibels) and the standard deviation were computed so as to determine stability and dependability of the findings.

The measurements were all made in ambient laboratory conditions and the approach of the methodology enabled a clear comparison of acoustic transmission properties of the reinforced composites as compared to the unmodified UPE matrix. This multi-frequency acoustic experiment method offered relevant

information on the sound-muffling properties of the UPE/HDPE composite materials, and their potential as sustainable sound insulating materials in the engineering field. The pictures of the tested specimens pretest and posttest may be considered in Supplementary Figure S5.

3. Results and Discussion

The FTIR spectroscopy was used to assess the chemical stability and structural integrity of HDPE that was subjected to thermal melting. In Fig. (3), the FTIR spectra of HDPE were obtained prior to and following the melting process and some possible changes in the spectrum or intensity could have been evidence of oxidation, degradation, or structural rearrangement.

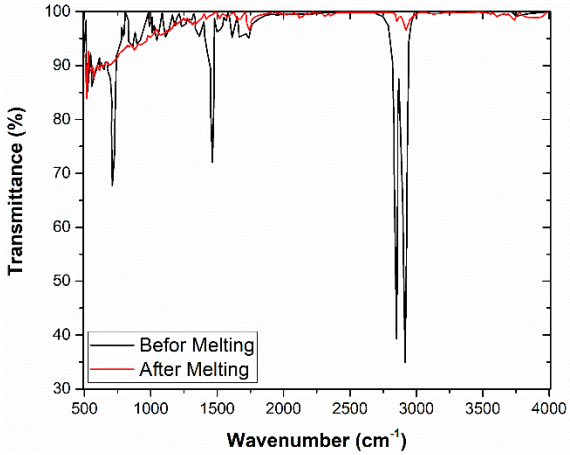

Fig. (3) FTIR of HDPE both before and after melting

HDPE shows very clear and sharp bands in the pre-melt spectrum, which are characteristic of semi-crystalline polyolefins. The prominent absorption peaks are:

- 2916 cm^{-1} and 2849 cm^{-1}: asymmetric and symmetric C-H stretch vibrations of methylene (-CH_2-) groups.
- ~1470 cm^{-1} and ~1462 cm^{-1}: indicative of CH_2 bending and scissoring modes.
- ~730–720 cm^{-1}: representing rocking vibrations of –CH_2– groups, characteristic of long methylene sequences in crystalline domains.
- ~1377 cm^{-1}: associated with CH_3 symmetric deformation.

After the analysis of the post-melting spectrum, the main bands remain mainly intact by the FTIR spectrum, which confirms the chemical stability and preservation of HDPE backbones under the thermal conditions used. Nonetheless, there are a number of significant changes which can be noted:

1- There is a general loss in peak intensity-particularly at 1465 cm^{-1} and 730 cm^{-1}, which is experienced following melting. This can be an indication of a partial loss of crystallinity, which does not contradict chain mobility and rearrangement during melting [31]. These are typical of semi-crystalline thermoplastics and do not always reflect the presence of chemical degradation.

2- Small changes in CH stretching (e.g., from 2916 to 2921 cm^{-1}) and CH2 bending modes can be caused by conformational rearrangements or changes in the arrangement of the molecules in solution [32]. These changes are indications of differences in the intermolecular interactions when the polymer chains realign after melting.

3- The broad band in the range of about 3600-3000 cm^{-1} -OH groups or moisture absorption is a little clearer in the post-melting spectrum. This can indicate may imply slight surface oxidation or adsorbed atmospheric moisture following melting and cooling [33] but the total transmittance is high.

4- Significantly, there are no additional peaks in the 1700-1800 cm^{-1} (characteristic of C=O stretching in oxidized polyethylene) ones. This confirms that there was no serious oxidative degradation [34], which suggests that the melting was done under conditions that ensured the integrity of the polymer (i.e. low oxygen atmosphere or inert atmosphere).

Taken together, these spectral measurements prove that the structure of the hydrocarbons core of HDPE has not been changed chemically due to melting. The minor changes in the intensity and the position of the absorption bands are the main signs of the physical changes, which may be a change in crystallinity, molecular ordering, or subtle conformational dynamics. The results are consistent with the existing literature on thermally processed polyethylenes, which reveal that HDPE does not lose its chemical identity during melting but its morphological and crystalline properties can change.

To evaluate the surface morphology of UPE composite prior to and after reinforcement using recycled HDPE particles, optical microscopy was used to aid in gaining microstructural understanding of the physical integration and dispersion of the filler phase. The micrographs, as provided in Fig. (4), provide a qualitative analysis of the surface features which give the underlying differences in material structure.

Figure (4a) indicates that the unreinforced UPE matrix contains a smooth, continuous, and nearly featureless surface, as would be expected of an isotropically cured thermosetting resin. The lack of clear inclusions or morphological abnormalities indicates a homogenous polymer structure, free of any secondary stage or interfaces. This morphology is characteristic of dense, crosslinked matrices and is consistent with high flexural strength and brittle fracture behavior in mechanical testing. The absence of energy-dissipating interfaces also contributes to the high levels of sound transmission to be found in acoustic testing since smooth homogeneous media are generally effective in transmission of acoustic waves with low attenuation.

By contrast, figure (4b) demonstrates a significantly heterogeneous surface morphology in the UPE matrix after reinforcement with 10 wt.% HDPE. The micrograph shows a large number of light-scattering regions, which are micron-sized HDPE domains in the UPE matrix. These characteristics are irregularly shaped and randomly spaced, which means they are unevenly distributed but widespread throughout the thermoplastic filler. Introduction of HDPE significantly changes the topography of the surface resulting in a more complex morphology reminiscent of microstructural inhomogeneity at the particle-matrix interface. This has also been noted with HDPE-based composites where surface roughness and domains of fillers are higher as the filler loading is increased [35].

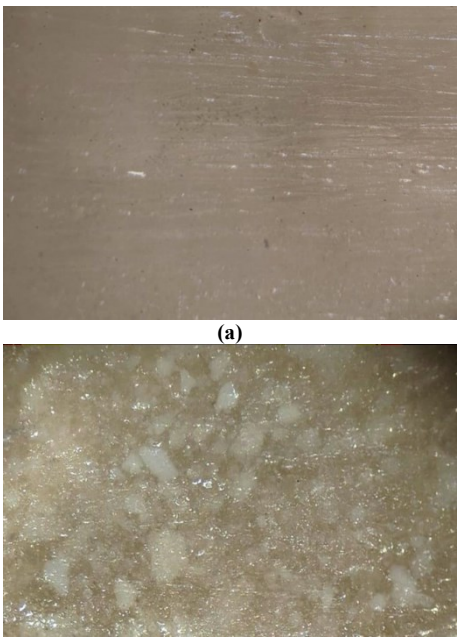

(a)

(b)

Fig. (4) (a) Surface morphology of the neat UPE matrix before reinforcement, exhibiting a smooth and homogeneous appearance, and (b) Surface morphology of the UPE composite reinforced with 10 wt.% HDPE, showing dispersed thermoplastic domains and increased surface heterogeneity due to particle–matrix interactions

The roughness of the surface and the distribution of the particles on Fig. (4b) can confirm the increased tendencies of the composite in acoustic damping since heterogeneous interfaces favor the scattering and dissipation of sound-waves. Scattering, absorption and reflection of acoustic waves at HDPE-UPE interfaces are the sources of the significant decrease in sound intensity that is transmitted, especially at higher frequencies. In addition, this interface-based morphology is also in line with the improved impact resistance and decreased flexural strength that have been reported on the composite. Although HDPE domains provide locations to dissipate energy during dynamic loading (impact), they are also possible sources of stress in the face of bending stress, which undermines load transfer across the composite network - as was previously observed with HDPE morphology and structural behavior as a whole [36].

Recycled HDPE in different proportions was added to UPE and the influence on the compressive strength studied. Figure 5 shows that compressive strength was very high with high content of HDPE. The average compressive strength of the neat UPE matrix was estimated as approximately 56.6 MPa that exhibits the common stiffness and brittleness of thermosetting resins. When HDPE concentration in the polymer was increased to 2.5 wt.%, a significant increment in the strength to 91.0 Mpa that equals 60.8% increment was detected. Addition of HDPE up to 10 wt.% further enhanced this trend with the maximum strength of 94.4 MPa recorded.

Such improvement in compressive performance may be explained by a number of interconnected factors. To begin with, inclusion of HDPE particles implies a heterogeneous phase which changes the distribution of stress during compressive loading. Although HDPE is a rather soft and ductile thermoplastic, it provides resist to energy dissipation and crack blunting that decrease the probability of catastrophic brittle fracture. Similar behavior can be observed with HDPE-based hybrid composites, where the toughness is increased through the absorption of fracture energy [37]. This enhanced load-bearing effect can probably be explained by the synergistic combined effect of rigid UPE matrix and tough, semi crystalline HDPE domains serving as stress redistribution during the axial loading. The ductile nature of HDPE enables it to experience the disastrous failure of matrix deformation in localized plastic deformation, which postpones by absorbing the energy of the compressive loads. These interactions not only facilitate the concentration of stress at the defects sites, but also make sure that many crack-arrest fronts are formed at the matrix, which is also supported by the small range of the standard deviation of the compressive test data.

In addition, the data has a high degree of reproducibility as showed by the small error bars of each data point in Fig. (5). Standard deviation of each group was small suggesting that there was tight control of the process and that there was uniform distribution of particles in all the fabricated samples. This uniformity supports the conclusion that the increases in compressive strength are not artifacts of sample variability, but are due to a strong, inherent increase of compressive strength as a result of HDPE reinforcement. The homogeneity also implies that the hand lay-up method, regardless of its simplicity, was successful in homogenous particle distribution at the micro level, which is a necessary requirement to ensure the reliability of mechanical behavior in particulate composites.

Microstructurally, the fracture mechanics of the compression of the polyester composite may also be

affected by the presence of HDPE particles within the polyester matrix. Whereas UPE is weak in crack propagation as it is brittle, HDPE particles may be used as crack-bridging particles or crack deflectors, lengthening the energy absorption ability of the material. This is especially applicable in compressive modes which the matrix is more vulnerable to buckling and shear failure, HDPE reinforcement inhibits such failure modes by deforming plastically and sharing loads [38]. It is however interesting to note that the compressive strength rate of increase starts to level off after 5 wt.% HDPE. This plateau effect can be achieved by the interactions between particles or particle clustering and can create weak spots or cause some local stress concentration- a similar effect has been observed in HDPE-based systems using natural or inorganic particulates [39]. With high filler loadings (e.g., 10 wt.%), there is a high chance of agglomeration, which is especially pronounced when there are no compatibilizers or surface treatment that enhance interfacial adhesion. As a result, the compressive strength keeps on increasing at 7.5 wt.% and 10 wt.% but the gains are smaller than those seen at lower HDPE contents.

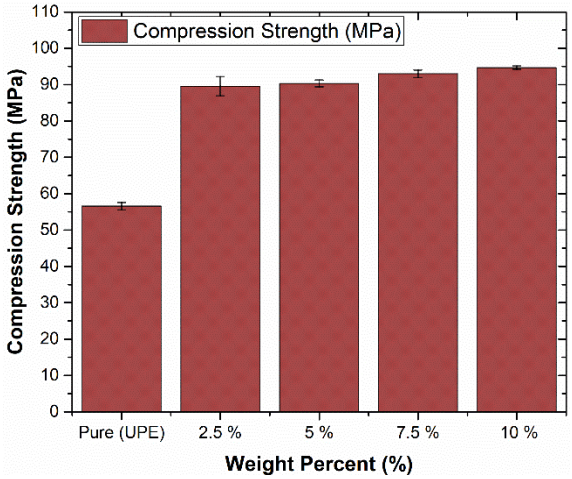

Fig. (5) Compressive strength of UPE / HDPE composites

The findings indicate the mechanical efficiency of using recycled HDPE particles as reinforcers in thermoset matrices. In addition to the technical advantages, the post-consumer HDPE usage is related to the sustainability, which is in line with the overall interests of the circular economy and waste valorization. However, further research is needed to explore the microstructural morphology (using SEM) and the interfacial chemistry (using Raman) as a way of further clarifying the reinforcement mechanism and optimizing the particle-matrix interface to increase the mechanical performance even further.

The effect on flexural strength of UPE composites by the addition of recycled HDPE particle reinforcement was systematically studied at five weight fractions, and the findings are shown in Fig. (6). The flexural strength of the unfilled UPE matrix was high, at about 165 MPa, which is typical of the stiff and brittle nature of thermoset polymers. However, with the addition of HDPE, a pronounced and consistent reduction in flexural performance was observed. The flexural strength sharply declined to 58.5 MPa and 59.2 MPa with the addition of 2.5 wt.% and 5 wt.% HDPE, respectively. Further increases to 7.5 wt.% and 10 wt.% led to even lower values of 27.6 MPa and 27.4 MPa, indicating an overall decline of more than 83% from the reference matrix.

The pronounced decline in flexural strength is governed by stress localization at weak HDPE–UPE interfaces. Under bending, tensile and shear components dominate the lower surface, and the ductile HDPE inclusions act as compliant zones where tensile stress cannot be effectively transferred. Unlike compressive loading, which distributes stress hydrostatically, flexure imposes differential tension–compression coupling that promotes interfacial decohesion and crack initiation around the low-modulus HDPE particles [40]. Hence, the same HDPE domains that redistribute compressive stress act as stress concentrators under bending, explaining the opposing mechanical responses observed.

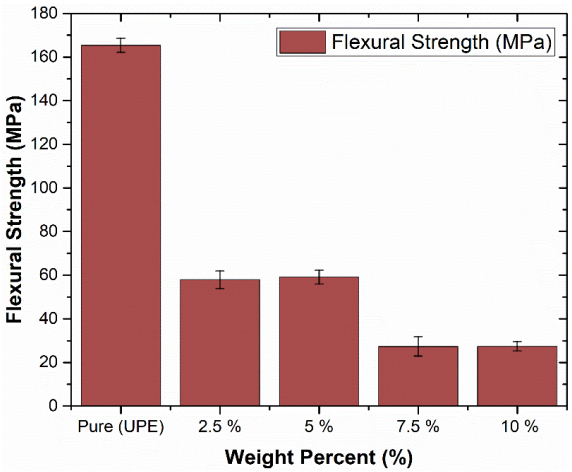

Fig. (6) Flexural strength of UPE / HDPE composites

Notably, figure (6) shows very narrow error bars on all the HDPE-containing samples because of the high reproducibility of the mechanical degradation. The small standard deviation indicates that the steep fall in flexural strength is not caused by processing anomalies, defects in the sample, or anomalies of filler clustering. Rather, it is a material reaction as a system, which is based on the poor interfacial adhesion and phase mismatch between the HDPE filler and thermosetting matrix. These results confirm that the flexural failure mode is controlled not only by the presence of a matrix crack, but also by the debonding of the particles, which are always re-producible in samples.

Micro-mechanically, it is found that the presence of HDPE alters the homogenous stress distribution on the

cross-section of the composite during flexure. These disruptions become more common and intense with the increase in HDPE content and limit the capacity of the matrix to transfer tensile stresses across its lower surface during bending. This is especially problematic considering that HDPE, as is (around 53 μm in diameter), is neither aligned to the stress direction, nor does it form a continuous reinforcement stage. Rather, the HDPE particles are soft inclusions that add negligible weight to structural stiffness and that might be stress risers, which accelerates crack propagation during flexural loading [41]. In addition, interfacial debonding witnessed in other comparable systems (reported in literature) is a probable factor in these findings. In the absence of compatibilization (e.g., silane coupling agents or functionalized HDPE), the bond between the particle and the matrix is poor, which compromises the stress transfer potential [42]. Unlike fiber-reinforced systems whereby the throughput of load is realized effectively across the interface, the HDPE particles here are more of passive fillers than active reinforcements. Furthermore, when loaded at higher agglomeration (7.510 wt.%) levels, there is the possibility of the agglomeration being clustered in form of micro voids or localization places of stress which serve as sites of initiation of flexural failure.

The findings of these results indicate that recycled HDPE can be effectively used to improve compressive strength but with a degree of caution in the application where a high degree of flexural integrity is required. To render such composites viable for bending-dominant applications, surface modification of the HDPE particles is essential to promote chemical compatibility and interfacial bonding. Plasma treatment, grafting with maleic anhydride or combining with compatibilizer resins could be used as important techniques to enhance the load transfer during bending and avoid premature failure of the interfaces.

This dynamic action of UPE composites under impact loading was considered as a function of the recycled HDPE particles content and the findings are graphically displayed in Fig. (7), with standard deviation error bars to indicate reproducible experimental behavior. The original UPE matrix had a mean impact strength of about 0.30 kJ/m^2, reflecting the brittle character of thermoset polyesters that generally fail via unstable crack propagation and low-energy absorption. When HDPE particles were incorporated a significant increase in impact strength was recorded especially at moderate filler contents indicating the toughening effect of the ductile thermoplastic phase.

The average impact strength was raised at the 2.5 wt.% and 5 wt.% HDPE to 0.42 and 0.43 kJ/m^2, respectively. This is because of the micro-mechanical energy dissipation processes that are imparted by the dispersed HDPE domains that deform to plastic when collisions occur and thereby slow down the crack propagation process [43,44]. These are crack deflection, crack pinning and shearing of the matrix at the HDPE-matrix interface. The semi-crystalline structure of HDPE, with its strong elongation and energy dissipation, is useful in softening the cracks and keeping the damages near the tip of the crack.

The maximum performance was met at a HDPE loading of 7.5 wt.% because the impact strength was 0.51 kJ/m^2. At this level of concentration, the reinforcement is easily diffused throughout the structure and enhances the interaction between reinforcing material and polymer matrix. Based on data, it is clear that HDPE particles were well dispersed and capable of relieving stress following a uniform distribution without generating phase discontinuity or clustering. This increased rigidity is consistent with past research on thermoplastic-filled thermosets, in which impact-induced failure is prevented by energy-absorbing fillers [45]. Further addition to 10 wt.% HDPE, however, resulted in a significant decrease in impact strength down to about 0.26 kJ/m^2. This excessive reduction can be explained by the agglomeration of particles, debonding of interfaces and ineffective wetting of filler surfaces, which combined create weak points that act as favored locations of crack propagation [46]. With such a high filler content, the structural integrity of the matrix is discontinued and the nature of the matrix in spreading impact forces evenly is undermined. In addition, the low chemical affinity between the hydrophobic HDPE particles and the polar UPE matrix further increases interfacial weaknesses especially when it is not treated with any surface treatment or compatibilizing agent.

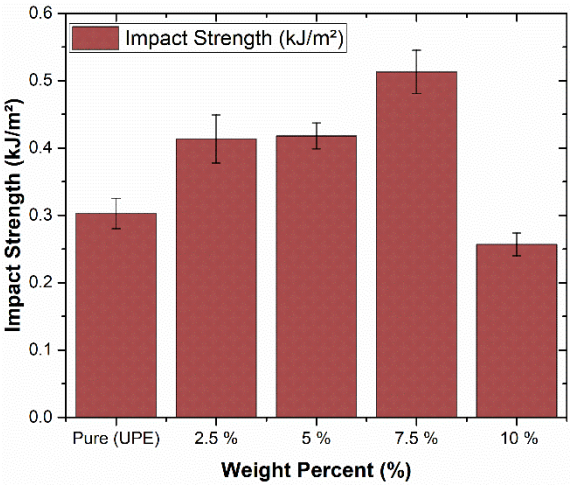

Fig. (7) Impact Strength of UPE / HDPE composites

The error spreads in Fig. (7) are also comparatively small in all compositions, which indicates a high level of reproducibility and consistency of the process. The slight increase in variability at 7.5 wt.% could be related to the transitional behavior at the optimum toughness point when competing mechanisms of crack

toughening and phase separation co-exist. Conversely, the decreased variability at 10 wt.% suggests that the failure mode is homogenous - probably brittle fracture due to interfacial debonding or particle-induced voids.

The fracture surfaces of UPE composites were assessed in optical microscopy prior to and after reinforcement with HDPE, in the presence or absence of dynamic loading. The comparative images in Fig. (8) give us an insight into the underlying fracture mechanisms which govern material performance under impact.

The fracture surface of the neat UPE matrix before impact testing as depicted in Fig. (8a) is usually flat and smooth, with a reflection surface, as a result of brittle mode of fracture. The lack of microvoids, shear deformation, or particulate disruption indicates that the polymer network ruptures through a fast crack propagation by a rigid and crosslinked network. This brittle behavior is also in line with the low impact energy absorption of mechanical testing and is characteristic of unsaturated polyesters in their neat state [47].

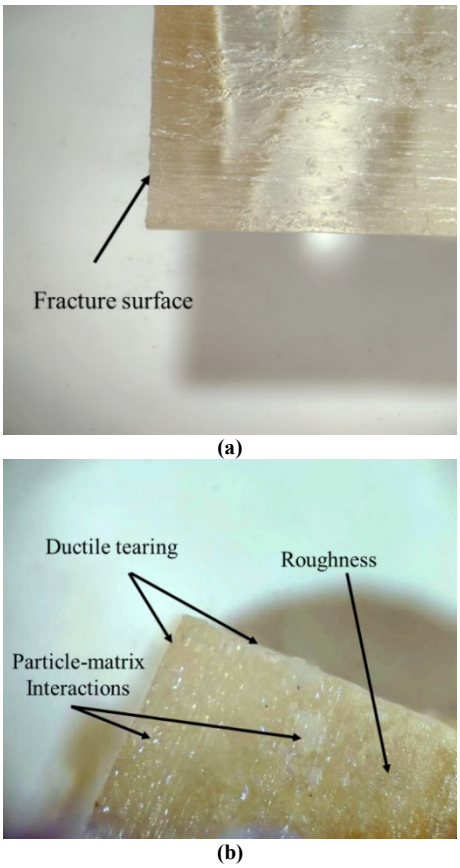

Fig. (8) (a) Fracture surface of neat UPE sample before impact testing, showing a smooth and brittle fracture profile, and (b) Fracture surface of UPE composite reinforced with 10 wt.% HDPE after impact testing, exhibiting increased roughness, particle-matrix interactions, and ductile tearing features (Magnification: ×40)

On the contrary, figure (8b) shows the fracture surface of a UPE composite reinforced with 10 wt.% HDPE after impact testing. The surface morphology becomes apparent, and rough areas, localized tears, and light-scattering areas appear. The characteristics indicate a ductile fracture process that occurs with the presence of HDPE domains that seem to have caused the crack blunting and plastic deformation during failure [48]. The ruggedness and discontinuity indicate energy loss by matrix stretching, filler-attachment loss, and interfacial friction-mechanisms absent in the unreinforced matrix.

The trends seen in the impact strength data are confirmed by the observed variations between the two surfaces of fracture: the neat UPE collapses catastrophically when subjected to dynamic loading, but the HDPE-based system exhibits greater energy-absorbing characteristics through microstructural toughening mechanisms. Moreover, the failure mode of the composite shows the presence of arrest and deflection of the cracks, which validates the reinforcing effect of HDPE regardless of its low interfacial bonding with UPE [49].

The Shore D scale was used to measure hardness levels of UPE composites that were reinforced with recycled HDPE particles to determine the surface resistance of the material to localized deformation. The findings, as shown in Fig. (9), suggest a steady increase in hardness as HDPE content increases to 5 wt.%, then the trend levels off. The UPE neat matrix had a mean hardness of 75.39±0.44, which is rather hard and cross-linked thermoset material with a low plastic deformation ability.

When HDPE was incorporated at 2.5 wt.%, the hardness rose to 78.28±0.45 and then more significantly reached 80.54±0.41 at 5 wt.%. This performance improvement is credited to the addition of dispersed HDPE particles, which, despite the fact that it is a less rigid thermoplastic than UPE, enhance local stiffness and penetration resistance of the composite by a mechanically locking mechanism. The semi-crystalline HDPE dispersed structures also act to inhibit surface deformation and stiffen the matrix at the micro-scaling level and thus tend to hinder localized indentation under the Shore D test conditions [41,50]. On increasing the loadings (7.5 and 10 wt.%), the hardness values became stagnant at 80.28±0.16 and 80.05±0.56 respectively. This effect of saturation implies that the composite system has a threshold point of filler effectiveness beyond which extra HDPE would not add a significant amount to further surface reinforcement. This plateau may be caused by a number of factors. Firstly, the agglomeration of the filler due to the increase of the loading can decrease the uniform dispersion and can introduce microvoids or diminish the continuity of the matrix [51]. Secondly, HDPE is soft relative to the UPE matrix, which restricts its

reinforcing effect in surface hardness when it reaches a high volume fraction.

The trend is further verified by the error bars in Fig. (9). The standard deviations were all low (not more than 0.56), as they indicated that the fabricated composites were reproducible and uniform. It is important to note that the least variability was at 7.5 wt.% HDPE (±0.16), and this suggests high-level consistency in surface properties and maybe because there was a properly developed dispersion phase at this intermediate level of filler. Conversely, a marginally greater variation at 10 wt.% indicates that there may be some localized irregularities in filler distribution or surface morphology, which is in line with the idea of overloading.

The impact of recycled HDPE reinforcement on the thermal conductivity of UPE composites was also investigated in a systematic manner and the outcomes are provided in Fig. (10). There is an apparent upward trend as the HDPE content increases, starting at 0.19 W/m.°C of unfilled UPE matrix and approaching 0.26 W/m.°C at 10 wt.% HDPE. This linear improvement indicates that the addition of HDPE adds a positive value to the heat conduction in the composite system, although this is only in small proportions with the low thermal conductivity that the two base materials have in nature.

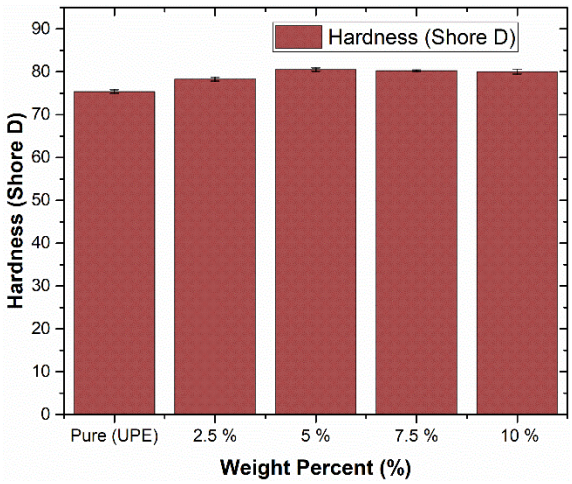

Fig. (9) Hardness of UPE / HDPE composites

Unreinforced UPE matrix is a thermoset polymer with a highly crosslinked structure and as such, it has low phonon mobility and high vibrational scattering, hence the low intrinsic thermal conductivity. But with introduction of recycled HDPE at 2.5 wt.% and 5 wt.%, it rises to 0.20 W/m.°C and 0.21 W/m.°C, respectively. The first enhancement may be explained by the fact that semi-crystalline HDPE domains are dispersed and that enhanced local structures are provided and phonon scattering is minimised as compared to the polymerised network of amorphous polymers [52]. Furthermore, the HDPE particles are less thermally resistant than voids or resin pockets, and thus offer additional conduction pathways, increasing the net energy flow.

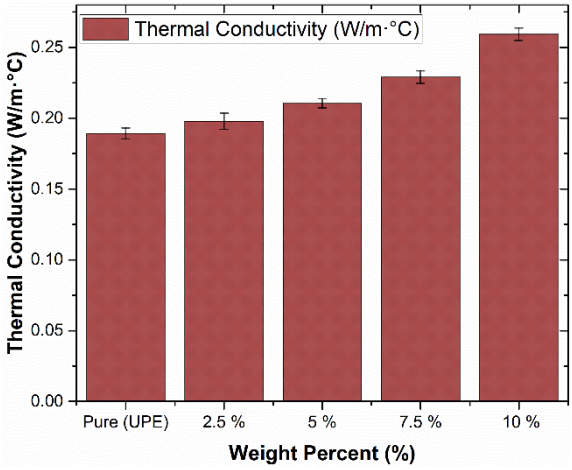

Fig. (10) Thermal conductivity of UPE / HDPE composites

Greater increases in HDPE loadings are seen at higher loads of 0.23 W/m.°C at 7.5 wt.% and 0.26 W/m.°C at 10 wt.%. Physically, the small increase in thermal conduction can be explained by a better phonon conduction along semi-crystalline HDPE domains that have lower scattering than the amorphous polyester network [53]. Inclusion of HDPE also reduces interfacial Kapitza resistance through the creation of continuous low-resistance channels, whereas the movement of chains in the cross-linked UPE is limited, limiting phonon mean free path. The resultant composite has a balance between phonon bridging and interface scattering that brings about an increase in conductivity.

The thermal behavior is also confirmed by the small standard deviation values seen in the plotted curves, which result in excellent reproducibility and uniformity of materials throughout all the formulations. Minor deviations at increased loading (mostly at 10 wt.%) can be explained by variability of microscale dispersions or slight agglomeration of HDPE particles. This type of clustering may cause local variations in particle connectivity, as well as in matrix–filler interfaces, both of which influence thermal flow behavior.

The observed increase in thermal conductivity of HDPE filled composites, though moderate, is important in the polymer matrix systems. This enhancement can be especially useful in non-structure applications demanding moderate heat dissipation or controlled thermal diffusion, like in electrical device enclosures, automotive interior cladding, or thermal insulation blankets in lightweight protective systems. Furthermore, the findings indicate how hybridization with high-conductivity fillers, including graphite, boron nitride, or aluminum oxide, can further enhance the heat transfer performance [54].

The acoustic insulation properties of UPE composites reinforced with recycled HDPE particles

were evaluated by determining the sound level (in dB) transmitted through the samples at 100 Hz, 1000 Hz, and 10000 Hz. As illustrated in Fig. (11), the results showed that there was a steady reduction in the intensity of sound that is transmitted as the HDPE content increased in all the tested frequencies, indicating that there is indeed a measurable improvement in the acoustic insulation behavior as a result of incorporating HDPE.

The pristine UPE matrix had the highest sound levels at all the frequencies, with mean values of 117.67 dB (100 Hz), 118.80 dB (1000 Hz), and 121.42 dB (10000 Hz). This is in line with the fact that unsaturated polyester resin is rigid and brittle and therefore it can transmit vibrational energy effectively due to its low damping factor. The introduction of 2.5 wt.% HDPE resulted in the significant decrease of the sound levels to 102.04 dB, 102.82 dB and 104.61 dB, respectively. This was observed with an upward trend in an increasing filler content with the lowest values of 98.71 dB, 99.24 dB, and 100.67 dB at 10 wt.% HDPE.

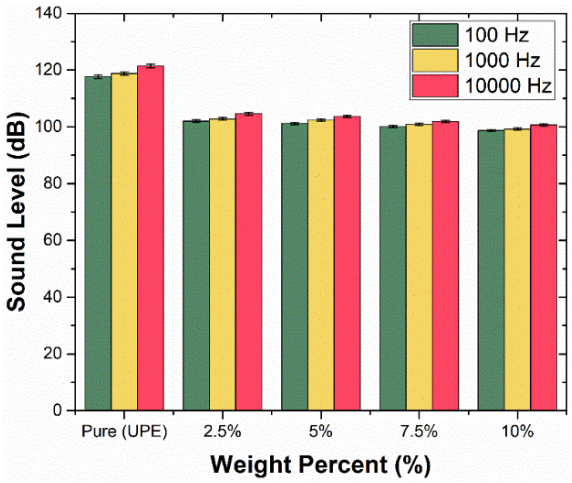

Fig. (11) Sound level measurements at 100, 1000, and 10,000 Hz for HDPE-reinforced UPE composites

This measured sound-pressure-level (SPL) has a threefold source, including (i) the mass-law contribution through the increased areal density (ii) viscoelastic damping by molecular friction of HDPE converting vibrational energy into heat (iii) the scattering of the wave by heterogeneous HDPE inclusions (~53 μm), which have dimensions comparable to the acoustic wavelength spanning mid-high frequencies (~10 GHz). All these effects have the beneficial effect of improving acoustic attenuation, which confirms the multifunctional nature of recycled HDPE as a damping and scattering agent [11]. They are especially intense at higher frequencies, where the shorter wavelength is more sensitive to fine-scale structural inhomogeneity, as seen in the difference of 20.7 dB between 0 wt.% and 10 wt.% HDPE at 10000 Hz. This shift was observed in testing of HDPE/SBR as well as HDPE/rubber composites using the impedance tube technique [55].

Notably, the obtained data are backed up by feasible standard deviations, which also contribute to the authenticity of the sound patterns. The standard deviations at 100 Hz varied between ±0.58 dB (unfilled matrix) and ±0.35 dB (10 wt.% HDPE), which is good repeatability of measurements and homogeneity of the sample behavior. The same trends were recorded at 1000 Hz (±0.61 to ±0.36 dB) and 10000 Hz (±0.66 to ±0.38 dB) and variability was slightly higher in the neat matrix, which is more homogenous and rigid and thus provides less acoustic damping. The uniform reduction in standard deviations with the increase of the HDPE content, could be attributed to more effective sound attenuation as well as even distribution of fillers throughout the polymer network.

Such results indicate that UPE/HDPE composites are frequency dependent acoustic attenuators, which have a great potential as wideband sound silencers. Optimization of their performance can be further achieved by changing the levels of HDPE loading or using hybrid fillers like rubber granules, foamed particles, or fibrous materials [56]. It can be used as applications in building partitioning, automotive interiors, packaging materials, or even sound absorbing panels to consumers and industrial. In this study, acoustic Insulation or Sound Transmission Loss (STL) was measured to evaluate acoustic insulation between two rooms according to the required applications. The Sound Pressure Level (SPL) was measured in the source room (L_1) and the receiving room (L_2), and the difference ($\Delta L = L_1 - L_2$) represents acoustic insulation in decibels (dB). It is worth noting that when evaluating sound absorption within a single room, the sound absorption coefficient (α) is used, which is related to the Noise Reduction Coefficient (NRC) and helps reduce echo and reverberation.

4. Conclusions

The present study demonstrated that incorporating recycled HDPE particles (≤10wt.%) into UPE significantly improved the composite's multifunctional performance while maintaining environmental sustainability. The compressive strength, impact strength, and surface hardness were improved, indicating enhanced load-bearing and surface rigidity. The thermal conductivity increased while acoustic insulation improved confirming more effective phonon and sound-wave attenuation. In contrast, the flexural strength declined due to weak interfacial adhesion between the polar UPE and non-polar HDPE phases. The chemical stability of recycled HDPE after remelting and the heterogeneous morphology were confirmed, which facilitated increased energy dissipation and damping. In general, the findings confirm recycled HDPE as an inexpensive, lightweight and environmentally-friendly filler that can be used in

non-structural applications, such as acoustic panels, vibration-damping parts and packaging.

References

[1] M. Álvarez et al., "Initiative to Increase the Circularity of HDPE Waste in the Construction Industry: A Physico-Mechanical Characterization of New Sustainable Gypsum Products", *Appl. Sci.,* 14(2) (2024) 478.

[2] V.A.P.M. Teixeira and L.S. De Moraes, "Post-consumer PET/HDPE blends as an alternative route for marketing recycled materials," *Concilium,* 23(18) (2023) 433-440.

[3] I.B. Valdivia, B.E.M. Medina and C.S. Mendoza, "Circular economy approach to recycling of high-density polyethylene (HDPE) for the production of pet products", *Sapienza: Int. J. Interdiscip. Stud.,* 5(2) (2024) e24036.

[4] J. Inga-Lafebre et al., "Preparation and characterization of a sustainable foamed biocomposite from compatibilized recycled polyethylene and agave fiber", *Polym. Bull.,* 81 (2024) 13071-13087.

[5] R. Meys et al., "Towards a circular economy for plastic packaging wastes – the environmental potential of chemical recycling", *Resour. Conserv. Recycl.,* 162 (2020) 105010.

[6] W. Cao et al., "The HDPE composites reinforced with waste hybrid PET/cotton fibers modified with the synthesized modifier", *e-Polymers,* 22 (2021) 30-37.

[7] J.-F. Liang et al., "Super toughness and reinforcement of recycled high-density polyethylene/poly(ethylene terephthalate) composite achieved by oriented spherical crystal structure", *Compos. B: Eng.,* 294 (2025) 112158..

[8] [4] O.A. Hammadi, "Fluorescence Characteristics of Random Gain Media Fabricated from Fluorescein Dye Containing Zinc Oxide Nanoparticles in Transparent Organic Hosts", *Iraqi J. Mater.,* 5(1) (2026) 47-52.

[9] Z.G. Wang et al., "Preparation and Properties of Recycled PET Fibers Filled Polyethylene Composites", *Mater. Sci. Forum,* 848 (2016) 89-93.

[10] A. Hellati and S. Boufassa, "Evaluation of the Role of Ethylene Vinyl Acetate on the Thermo-Mechanical Properties of PET/HDPE Blends", *Eng. Technol. Appl. Sci. Res.,* 12(6) (2022) 9546-9550.

[11] B. Haworth et al., "Thermoplastic composite beam structures from mixtures of recycled HDPE and rubber crumb for acoustic energy absorption", *J. Thermoplast. Compos. Mater.,* 31 (2018) 119-142.

[12] A.A. Reguig, S. Bouhelal and R. Doufnoune, "Optimizing high-density polyethylene (HDPE) performance: utilizing diatomaceous earth filler and an innovative reversible crosslinking reaction agent (RXR)", *J. Mater. Sci.,* 59 (2024) 11346-11361.

[13] A. Wu et al., "Preparation and Finite Element Analysis of Fly Ash/HDPE Composites for Large Diameter Bellows", *Polymers,* 13(23) (2021) 4204.

[14] S. Satapathy and R. Kothapalli, "Mechanical, Dynamic Mechanical and Thermal Properties of Banana Fiber/Recycled High Density Polyethylene Biocomposites Filled with Flyash Cenospheres", *J. Polym. Environ.,* 26 (2017) 200-213.

[15] B. Neher et al., "Study of the Physical, Mechanical and Thermal Properties of Banana Fiber Reinforced HDPE Composites", *Mater. Sci. Appl.,* 11(4) (2020) 245-262.

[16] A. Rubiano-Navarrete et al., "Effect of Fiber Loading on Green Composites of Recycled HDPE Reinforced with Banana Short Fiber: Physical, Mechanical and Morphological Properties", *Polymers,* 16(23) (2024) 3299.

[17] P. Pereira et al., "Characterization of High Density Polyethylene (HDPE) Reinforced with Banana Peel Fibers", *BioResources*, 8(2) (2013) 2351-2365.

[18] A.L. Catto et al., "Influence of coupling agent in compatibility of post-consumer HDPE in thermoplastic composites reinforced with eucalyptus fiber", *Mater. Res.,* 17 (2014) 203-209.

[19] L. Zhong-xiang, "In-situ compatibilization of HDPE/wood fiber composites", *J. Central South Univ. Forest. Technol.,* 1 (2012) 122-125.

[20] K. Charoensri, Y. Shin and H. Park, "Innovative HDPE Composites Enriched with UV Stabilizer and Diatomaceous Earth/Zinc Oxide for Enhanced Seafood Packaging and Antimicrobial Properties", *Polymers,* 15(23) (2023) 4577.

[21] M.H.M. Sayuti et al., "Development of marine grade radiation cross-linked high density polyethylene (HDPE) floater pontoon material", *IOP Conf. Ser.: Mater. Sci. Eng.,* 785 (2020) 012033.

[22] M.W. Khan et al., "Mechanical and UV stability of HDPE composites reinforced with carbon black and zinc oxide for solar floater applications", *Prog. Rubber Plastics Recycl. Technol.,* doi: 10.1177/14777606251316037.

[23] B. Alshammari et al., "Impact of Hybrid Fillers on the Properties of High Density Polyethylene Based Composites", *Polymers,* 14(16) (2022) 3427.

[24] M. Zimmermann et al., "Evaluation of the degradation of HDPE hybrid composites using wood flour from CCA-treated poles, and recycled ceramic insulators", *J. Thermoplast. Compos. Mater.,* 32 (2018) 1677-1690.

[25] S. T. Peters, **"Handbook of Composites"**, 2nd ed., Springer (NY, 2013).
[26] ASTM International, "Standard Test Methods for Flexural Properties of Unreinforced and Reinforced Plastics and Electrical Insulating Materials", *ASTM D790-25* (2023), doi: 10.1520/D0790-25.
[27] ASTM International, "Standard Test Method for Compressive Properties of Rigid Plastics", *ASTM D695-26* (2023), doi: 10.1520/D0695-26.
[28] ASTM International, "Standard Test Method for Determining the Charpy Impact Resistance of Notched Specimens of Plastics", *ASTM D6110-18* (2018), doi: 10.1520/D6110-18.
[29] ASTM International, "Standard Test Method for Rubber Property—Durometer Hardness", *ASTM D2240-15* (2021), doi: 10.1520/D2240-15R21.
[30] V.M. Barragán et al., "Testing a simple Lee's disc method for estimating throuh-plane thermal conductivity of polymeric ion-exchange membranes", *Int. J. Heat Mass Transfer,* 184 (2022) 122295.
[31] H. Zheng et al., "Study on Crystallization Kinetics of Partially Melting Polyethylene Aiming To Improve Mechanical Properties", *Ind. Eng. Chem. Res.,* 53 (2014) 6211-6220.
[32] T. Bayerl et al., "Thermal degradation analysis of short-time heated polymers", *J. Thermoplast. Compos. Mater.,* 28 (2015) 390-414.
[33] G. George et al., "Real-time analysis of the thermal oxidation of polyolefins by FT-IR emission", *Polym. Degrad. Stability,* 48 (1995) 199-210.
[34] A. Cuadri and J. Martín-Alfonso, "The effect of thermal and thermo-oxidative degradation conditions on rheological, chemical and thermal properties of HDPE", *Polym. Degrad. Stability,* 141 (2017) 11-18.
[35] F.J.H.T.V. Ramos and L.C. Mendes, "Recycled high-density polyethylene/gypsum composites: evaluation of the microscopic, thermal, flammability, and mechanical properties", *Green Chem. Lett. Rev.,* 7 (2014) 199-208.
[36] Z. Bałaga et al., "AFM Measurements and Testing Properties of HDPE and PBT Composites with Fillers in the Form of Montmorillonite and Aluminum Hydroxide", *Materials,* 15(24) (2022) 8738.
[37] R. Girimurugan et al., "An experimental study on compressive properties of high density polyethylene-nano alumina-groundnut shell hybrid composites", *Mater. Today: Proceed.,* 68(6) (2022) 2226-2232..
[38] A. Pandey, E. Jan and P. Aswath, "Physical and mechanical behavior of hot rolled HDPE/HA composites", *J. Mater. Sci.,* 41 (2006) 3369-3376.
[39] B. Ayyanar et al., "Effect of natural fillers as reinforcements on mechanical and thermal properties of HDPE composites", *J. Thermoplast. Compos. Mater.,* 37 (2023) 800-819.
[40] S. Singh et al., "Tensile and Flexural Behavior of Hemp Fiber Reinforced Virgin-recycled HDPE Matrix Composites", *Procedia Mater. Sci.,* 6 (2014) 1696-1702.
[41] B. Aldousiri, M. Alajmi and A. Shalwan, "Mechanical Properties of Palm Fibre Reinforced Recycled HDPE", *Adv. Mater. Sci. Eng.,* 2013 (2013) 1-7.
[42] D.R. Mulinari, A.J.F. Marina and G.S. Lopes, "Mechanical Properties of the Palm Fibers Reinforced HDPE Composites", *Int. J. Chem. Mole. Eng.,* 103 (2015) 903-906.
[43] A. Sayem et al., "Thermoplastic Composites reinforced with Multi-layer Woven Jute Fabric: A Comparative Analysis", *Adv. Mater. Process. Technol.,* 8 (2020) 355-379.
[44] M. Kazemi et al., "Low-velocity impact behaviors of a fully thermoplastic composite laminate fabricated with an innovative acrylic resin", *Compos. Struct.,* 250 (2020) 112604.
[45] F. Hanan et al., "Characterization of Hybrid Oil Palm Empty Fruit Bunch/Woven Kenaf Fabric-Reinforced Epoxy Composites", *Polymers (Basel),* 12(9) (2020) 2052.
[46] A. Ünal et al., "Determination of the Effects of Recycling on Polyolefin Matrix Composites", *9th Int. Conf. Compos. Sci. Technol. (ICCST/9),* (2013).
[47] S. Thalib, "Fracture Surface of Polyester/Areca Nut Fiber Composite Under Impact and Tensile Loading", *Int. J. Emerg. Trends Eng. Res.,* 8(6) (2020) 2523-2528.
[48] X. Zhuang and X. Yan, "Investigation of damage mechanisms in self-reinforced polyethylene composites by acoustic emission", *Compos. Sci. Technol.,* 66 (2006) 444-449.
[49] Y. Guo et al., "Analysis and Identification of the Mechanism of Damage and Fracture of High-Filled Wood Fiber/Recycled High-Density Polyethylene Composites", *Polymers,* 11(1) (2019) 170.
[50] A. Boussetta et al., "Effect of Cellulose Microfibers from Sugar Beet Pulp By-product on the Reinforcement of HDPE Composites Prepared by Twin- screw Extrusion and Injection Molding", *J. Bionic Eng.,* 20(1) (2023) 349-365.
[51] A. Koffi, D. Koffi and L. Toubal, "Mechanical properties and drop-weight impact performance of injection-molded HDPE/birch fiber composites", *Polym. Test.,* 93 (2021) 106956.
[52] W. Zhou et al., "Thermal conductivity of boron nitride reinforced polyethylene composites", *Mater. Res. Bull.,* 42 (2007) 1863-1873.
[53] M. Kole, D. Tripathi and T. Dey, "Percolation based enhancement in effective thermal

conductivity of HDPE/LBSMO composites", *Bull. Mater. Sci.,* 35 (2012) 601-609.
[54] J. Che et al., "Largely improved thermal conductivity of HDPE/expanded graphite/carbon nanotubes ternary composites via filler network-network synergy", *Compos. A: Appl. Sci. Manufact.,* 99 (2017) 32-40.
[55] X. Xu et al., "Sound absorbing properties of perforated composite panels of recycled rubber, fiberboard sawdust, and high density polyethylene", *J. Cleaner Product.,* 187 (2018) 215-221.
[56] A.I. Nigmatullina et al., "Sound-Absorbing Polymer Composite Materials for Construction Purposes", *IOP Conf. Ser.: Mater. Sci. Eng.,* 753(5) (2020) 052027.

5. Supplementary Materials

To support the main findings presented in this study, a series of photographs of the experimental specimens before and after mechanical, thermal, and acoustic testing are included in this Supplementary Section. These images provide visual confirmation of the specimen geometries, failure modes, and test-specific configurations used throughout the evaluation of UPE/HDPE composites.

5.1 Figure S1. Flexural Test Specimens – Before and After Testing

The visual comparison of flexural test specimens is provided to illustrate the dimensional consistency and fracture behavior observed after three-point bending tests.

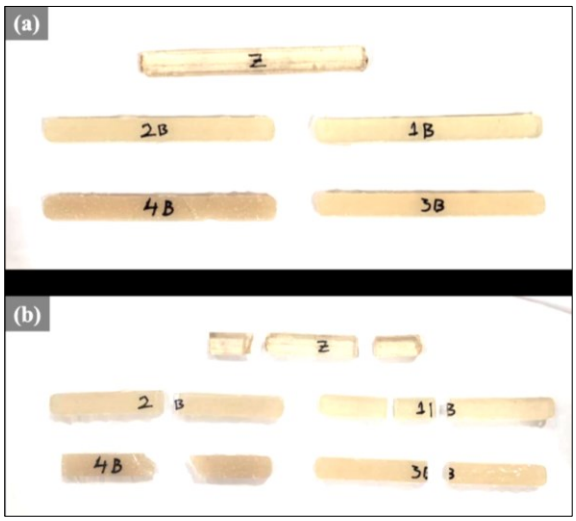

Fig. (S1) Flexural test specimens before and after testing. The figure shows the five UPE/HDPE composite samples labeled Z (0% HDPE), 1B (2.5%), 2B (5%), 3B (7.5%), and 4B (10%). The top row displays the untested specimens, while the bottom row shows their corresponding fracture modes after flexural loading. The results visually demonstrate increasing flexibility and improved fracture resistance with higher HDPE content

5.2 Figure S2. Compressive Test Specimens – Before and After Testing

This figure presents the appearance of the composite cubes before and after undergoing compressive strength testing. The comparison highlights the deformation behavior associated with different HDPE concentrations.

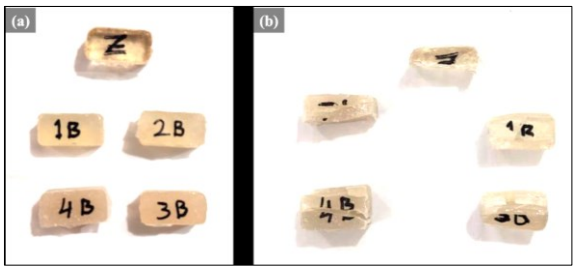

Fig. (S2) Compressive test specimens: pre- and post-test conditions. Subfigure (a) depicts the initial condition of the five UPE/HDPE specimens, while subfigure (b) shows the failed specimens following compression testing. The labels (Z, 1B, 2B, 3B, 4B) represent increasing HDPE weight fractions. Notable crushing and cracking are evident in low-HDPE samples, while higher HDPE formulations show more ductile collapse patterns.

5.3 Figure S3. Charpy Impact Specimens – Before and After Testing

Images of the impact specimens before and after Charpy testing are presented to visualize the variation in fracture surface and notch response among the tested composites.

Fig. (S3) Charpy impact test specimens before and after testing. Subfigure (a) shows the original notched specimens labeled Z to 4B, and subfigure (b) displays the fractured segments after testing. The progressive change in fracture pattern from brittle to ductile confirms the increased toughness imparted by HDPE inclusion, especially beyond 5 wt.%

5.4 Figure S4. Specimens for Shore D Hardness and Thermal Conductivity Tests

This figure shows the disk-shaped samples used to perform both Shore D hardness and thermal conductivity measurements, ensuring geometric consistency across the tests.

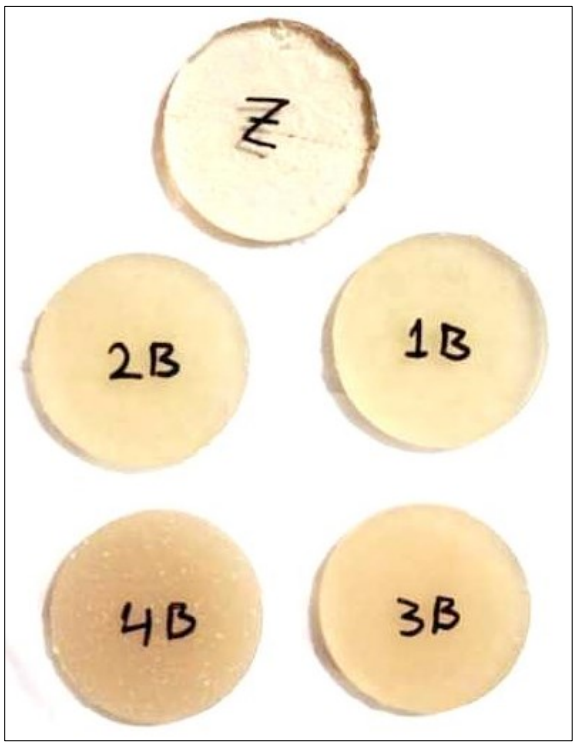

Fig. (S4) Disk-shaped specimens used for Shore D hardness and thermal conductivity testing. Each circular specimen (Z to 4B) was tested under identical environmental and loading conditions. Their uniform dimensions were chosen to ensure reliable comparisons of mechanical hardness and heat conduction performance as a function of HDPE content

5.5 Figure S5. Acoustic Insulation Specimens

The acoustic panels prepared for sound insulation evaluation are displayed below. These samples were tested in a reverberation chamber setup to assess noise attenuation across a range of frequencies.

Fig. (S5) Acoustic insulation test specimens. This figure includes the square panels of UPE/HDPE composites labeled Z (0%), 1B (2.5%), 2B (5%), 3B (7.5%), and 4B (10%). These were installed as barriers in the acoustic test rig to quantify reductions in sound pressure levels at 100 Hz, 1000 Hz, and 10,000 Hz. The visual consistency supports the validity of the acoustic data reported in the main text

